On transition to bursting via deterministic chaos

Georgi S. Medvedev *

February 6, 2008

Abstract

We study statistical properties of the irregular bursting arising in a class of neuronal models close to the transition from spiking to bursting. Prior to the transition to bursting, the systems in this class develop chaotic attractors, which generate irregular spiking. The chaotic spiking gives rise to irregular bursting. The duration of bursts near the transition can be very long. We describe the statistics of the number of spikes and the interspike interval distributions within one burst as functions of the distance from criticality.

Bursting oscillations are ubiquitous in the experimental and modeling studies of excitable cell membranes. Many models generating bursting have been subject to intensive research due to their physiological significance and dynamical complexity (see [1, 5, 7, 9, 10, 13, 15] and references therein). Under the variation of parameters even minimal $3D$ models of bursting neurons exhibit a rich variety of periodic and aperiodic dynamical patterns corresponding to different spiking and bursting regimes. The transitions between these patterns may contain complex dynamical structures such as period-doubling cascades and deterministic chaos. In particular, it was shown that the transition from tonic spiking to bursting in a class of bursting neuron models, so-called square-wave bursters, contains windows of chaotic dynamics [1, 2, 10, 15]. In view of the complex bifurcation structure of this class of problems, it is important to identify the universal features pertinent to different dynamical patterns and transitions between them. In the present Letter, we describe statistical features of the irregular bursting arising in a class of neuronal models close to the transition from spiking to bursting. Prior to transition to bursting, the systems in this class develop chaotic attractors, which generate irregular spiking. The chaotic spiking gives rise to irregular bursting. The duration of bursts near the transition can be extremely long (see Figure 1). We analyze the statistics of the number of spikes and the interspike intervals within one burst as functions of the distance from criticality.

To describe our results, we use a three variable model of a bursting neuron introduced in [5]. The model is based on three nonlinear conductances: persistent sodium, I_{NaP}, the delayed rectifier, I_K, a slow potassium M-current, I_{KM}, and a passive current, I_L. In spite of a number of

*Department of Mathematics, Drexel University, 3141 Chestnut Street, Philadelphia, PA 19104, medvedev@drexel.edu

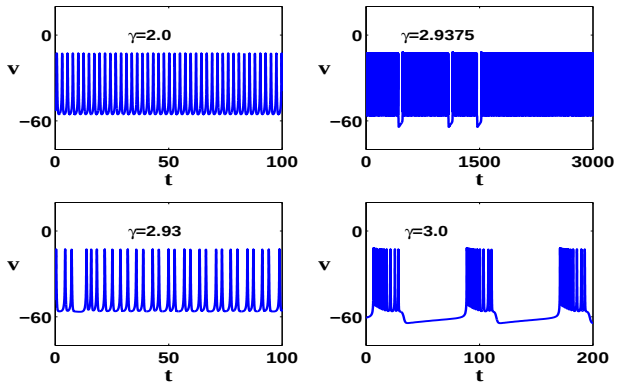

Figure 1: Periodic and aperiodic firing patterns generated by (1)-(3) in the regimes close to the transition from spiking to bursting. The values of parameters are $C = 1\ \left(\mu F cm^{-2}\right)$; $g_{NA} = 20$, $g_K = 10$, $g_L = 8\ \left(mS cm^{-2}\right)$; $E_{Na} = 60$, $E_K = -90$, $E_L = -80\ (mV)$; $a_m = -20$, $a_n = -25$, $a_w = -20\ (mV)$; $b_m = 15$, $b_n = 5$, $b_w = 5$; $\tau_n = 0.152$, $\tau_w = 20\ \left(ms^{-1}\right)$, and $I = 5pA$.

simplifications, the model captures essential features of a class of more detailed physiological models and is representative for a class of square-wave bursters [5]. The latter are among most common models of bursting. The following system of three differential equations describes the dynamics of the membrane potential, v, and two gating variables n and w:

$$C\dot{v} = F(v,n,w), \tag{1}$$

$$\dot{n} = \frac{n_\infty(v) - n}{\tau_n}, \tag{2}$$

$$\dot{w} = \frac{w_\infty(v) - w}{\tau_w}, \tag{3}$$

where $F(v,n,w) = -g_{NaP} m_\infty(v)(v - E_{NaP}) - g_K n(v - E_K) - \gamma w(v - E_K) - g_L(v - E_L) + I$; g_s and E_s, $(s \in \{NaP, K, L\})$ are the maximal conductance and the reversal potential of I_s, $s \in \{NaP, K, L\}$, respectively; and I is the applied current. The maximal conductance of I_{KM}, γ, is viewed as a control parameter. The time constants τ_n and τ_w determine the rates of activation in the populations of K and KM channels. The steady state functions are defined by

$$s_\infty(v) = \frac{1}{1 + \exp\left(\frac{a_s - v}{b_s}\right)}, \qquad s \in \{m, n, w\}\,.$$

The parameter values are given in the caption to Figure 1.

The analysis of the bursting neuron models like (1)-(3) uses a fast-slow decomposition [9, 5, 10]. Specifically, we note that the time constant τ_w presents the slowest time scale in the dynamics of (1)-(3). Therefore, we view $\alpha = \tau_w^{-1} > 0$ as a small parameter. In the limit as $\alpha \to 0$, system (1)-(3) is reduced to a $2D$ fast subsystem (1), (2), where w is viewed as a parameter. For values of $w \in (w_{AH}, w_{HC})$ the fast subsystem has a family of stable periodic orbits, which is born at the Andronov-Hopf bifurcation at $w = w_{AH}$ and terminates at the homoclinic bifurcation at $w = w_{HC}$.

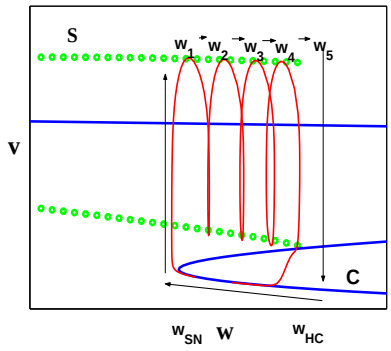

Figure 2: The bifurcation diagram of the fast subsystem (1) and (2) with a superimposed periodic trajectory induced by the slow equation (4). Curves S and C indicate the families of periodic orbits and the fixed points respectively.

A trajectory of the full system (1)-(3) approaches the surface foliated by the periodic orbits of the fast subsystem, S (Figure 2). The evolution along S is governed by the slow equation:

$$\dot{w} = \alpha \left(w_\infty(v) - w \right), \tag{4}$$

where the leading order approximation of $v(t)$ is obtained from the fast equations (1) and (2). When the trajectory hits the boundary of S (i.e., when $w > w_{HC}$), it jumps down to the curve of stable fixed points C, the only attracting set of the fast subsystem for $w > w_{HC}$. Then it evolves along C as shown in Figure 2 until it reaches the boundary of C at $w = w_{SN}$, corresponding to a saddle-node (SN) bifurcation in the fast subsystem. This is followed by the jump back to S and the oscillations in the fast subsystem resume. This description accounts for one cycle of bursting oscillation.

The description of bursting dynamics in a wide class of neuronal models, including (1)-(3), can be reduced to a single difference equation for the slow variable. Indeed, since the state of the fast system is determined by the value of the slow variable w, it is sufficient to know how w changes after each cycle of oscillations of the fast subsystem and after the period of quiescence:

$$w_{n+1} = P_\gamma \left(w_n \right), \; n = 1, 2, \ldots . \tag{5}$$

This idea underlies the method of reduction of a class of models of bursting neurons to one-dimensional maps proposed in [7]. Similar map-based approaches were used in [11] for studying bursting patterns in the Belousov-Zhabotinskii reaction and in [8] for analyzing complex oscillatory regimes in a compartmental model of the dopamine neuron. In [7], we provided the analytical description for P_γ, which was used to account for various spiking and bursting patterns and transitions between in the class of models of excitable cells. For the model at hand, the one-dimensional map is shown in Figure 3. The bifurcation structure of the fast subsystem endows the map with distinct structure: it is a piecewise continuous map with the boundary layer, I_0, corresponding to the homoclinic bifurcation in the fast subsystem (Figure 3). There are two intervals of continuity in the domain of definition of P_γ, $I_1 = I^- \bigcup I^0$ and $I_2 = I^+$. The iterations of P_γ over I_1 correspond to the changes of w after each spike of voltage and the definition of P_γ over I_2 captures

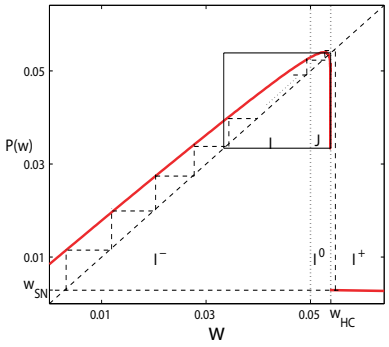

Figure 3: The first return map for the slow variable w for the value of control parameter $\gamma = 2.9375$ close to the critical value γ^c.

the mechanism of return to spiking after the period of quiescence (Figure 3). In I_2, $P_\gamma \approx w_{SN}$ is almost constant and can be well approximated by a linear function with a small negative slope (see Remark 5.3(b) in [7]). By construction, P_γ has a unique fixed point $\bar{w}_\gamma \in I_1$. For small values of γ, $\bar{w}_\gamma$ is globally attracting. The trajectory of (5) stays in a small neighborhood of $\bar{w}_\gamma \in I_1$ after several iterations of P_γ. Therefore, the value of w in (1) and (2) changes little and the fast subsystem generates periodic spiking. The bifurcation scenario described in [7] for a model of a bursting neuron applies to a wide class problems including (1)-(3). According to this scenario, for increasing values of γ the fixed point $\bar{w}_\gamma$ loses stability through a period-doubling (PD) bifurcation, giving rise to a stable period 2 orbit. In the continuous system (1)-(3), this corresponds to the appearance of the stable periodic solution formed by clustered pairs of spikes, so-called doublets. Under further increase of γ, the numerical experiments show other PD bifurcations of periodic orbits and, eventually, the dynamics of the discrete system (5) becomes chaotic. This scenario fits well with the numerical results reported for related models [1, 2, 7]. While the maximum of P_γ over I_1, $\bar{P}_\gamma = max_{w\in I_1} P_\gamma(w)$ remains less than w_{HC}, $P_\gamma(I_1) \subset I_1$, and the trajectories of (5) are trapped in I_1. This means that, in this regime, the continuous system exhibits (possibly chaotic) spiking. The transition to bursting takes place at $\gamma = \gamma^c$:

$$\bar{P}_{\gamma^c} = w_{HC}. \tag{6}$$

For $\gamma > \gamma^c$, trajectories of (5) may leave I_1. However, for values of γ just above γ^c, the window of escape, J_γ, is very small (see Figure 3). Therefore, a trajectory of (5) with large probability spends a long time in I_1 before escaping to I_2. If, in addition, the dynamics of (5) for $\gamma = \gamma_c$ has mixing property, the transition to bursting lies through regimes of chaotic bursting with very long intervals of spiking appearing with large probability. Below we study the statistics of the number of spikes and the interspike intervals within one burst for (1)-(3) near the transition to bursting.

Let $I = [w_0, w_{HC}]$, $w_0 = \lim_{w\to w_{HC}-0} P_\gamma(w)$ (see Figure 3) and assume that at the critical value of the control parameter $\gamma = \gamma^c$, map $P_{\gamma^c} : I \mapsto I$ has an invariant probability measure μ absolutely continuous to the Lebesgue measure on I. In addition, we assume that P_{γ^c} has the mixing property:

$$\lim_{n\to\infty} \mu\left(A \cap P_{\gamma^c}^{-n}(B)\right) = \mu(A)\mu(B), \tag{7}$$

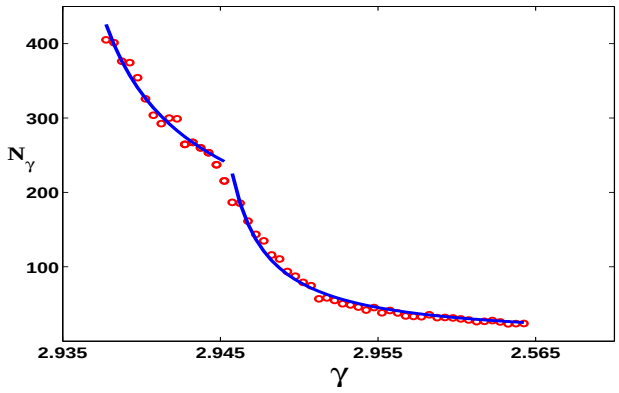

Figure 4: The mean values of the number of spikes, N_γ, are fitted with $y = a\left(\gamma - \gamma^c\right)^{\frac{-1}{2}}, (\gamma < \bar{\gamma})$ and $y = b\left(\gamma - \gamma^c\right)^{-1}, (\gamma > \bar{\gamma})$, where $a \approx 25.42$, $b \approx 0.52$, $\gamma^c \approx 2.93419$, and $\bar{\gamma} \approx 2.934343$.

for all measurable sets $A, B \subset I$ [14]. Let $\gamma - \gamma^c > 0$ be sufficiently small. Denote $\delta = \mu(J_\gamma)$, where $J_\gamma = \{w \in I :\ P_\gamma(w) > w_{HC}\}$ (Figure 3). Then the expected value (with respect to the probability measure μ) of the number of spikes within one burst is given by

$$N_\gamma = \mu(J_\gamma) + \sum_{k=2}^{\infty} k\mu_k, \tag{8}$$

where $\mu_k = \mu\left(P_\gamma^{-k+1}(J_\gamma) \bigcap \overline{\bigcup_{i=0}^{k-2} P_\gamma^{-i}(J_\gamma)}\right)$ and $\overline{A}$ stands for $I - A$. Let $m_k = \mu\left(\overline{\bigcup_{i=0}^{k-2} P^{-i}(J_\gamma)}\right)$ for $k \geq 2$. Then by mixing property (7), for sufficiently large $k_0 \in \mathbb{N}$,

$$\mu_k \approx \delta m_k \approx \delta m_{k_0}\left(1-\delta\right)^{k-k_0},\ k > k_0. \tag{9}$$

The combination of (8) and (9) yields

$$N_\gamma = \Sigma_{k_0} + m_{k_0}\delta \sum_{k=1}^{\infty}\left(k + k_0\right)\left(1-\delta\right)^{k-k_0}, \tag{10}$$

where Σ_{k_0} stands for the first k_0 terms on the right-hand side of (8). By taking into account, $\Sigma_{k_0} = O(1)$ and $\sum_{k=1}^{\infty}\left(k + k_0\right)\left(1-\delta\right)^k = O\left(\delta^{-2}\right)$, from (10) we obtain $N_\gamma = O\left(\delta^{-1}\right)$. In a small neighborhood around the point of maximum, the graph of P_γ is to leading order quadratic. Therefore, the size of the window J_γ, $\delta = \mu(J_\gamma) = O\left(\sqrt{\gamma - \gamma_c}\right)$, and $N_\gamma = O\left(\left(\gamma - \gamma^c\right)^{\frac{-1}{2}}\right)$. To estimate N_γ in a larger neighborhood of γ^c, we need to review certain facts about the structure of P_γ. It follows from the construction of P_γ in [7], that outside of the exponentially small neighborhood of w_{HC}, $\tilde{I}$, P_γ can be approximated by a linear map. This implies that for $\gamma > \bar{\gamma} = \gamma^c + O\left(e^{\frac{-C_1}{\alpha}}\right)$ the size of J_γ grows approximately linearly with γ, $\delta \approx O\left(\gamma - \bar{\gamma}\right)$ and $N_\gamma = O\left(\left(\gamma - \bar{\gamma}\right)^{-1}\right)$ for $\gamma > \bar{\gamma}$. Therefore, in the vicinity of γ^c, there are two regions of qualitatively distinct asymptotic behaviors of N_γ as a function of the distance from criticality. The numerical results shown in Figure 4 confirm this conclusion and clearly indicate the boundary between these two regions, $\bar{\gamma} \approx 2.943$.

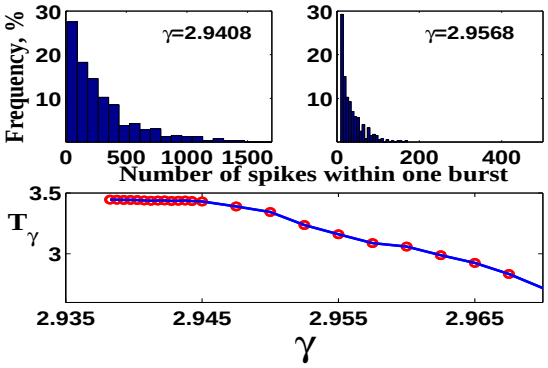

Figure 5: The histograms for the number of spikes within one burst and the mean values of the interspike intervals within one burst, T_γ.

The proposed mechanism for irregular bursting implies that near the transition to bursting, N_γ has a geometric distribution, whose parameters are determined by the width of the window of escape, J_γ (see Figure 5).

Next, we turn to estimating the expected value for the interspike intervals within one burst, T_γ. For small $\gamma - \gamma^c > 0$, we have

$$T_\gamma \approx \int_{I-J_\gamma} T\left(w, \gamma^c\right)\, d\mu(w), \tag{11}$$

where $T\left(w,\gamma\right)$ stands for the period of oscillations in the fast subsystem (1),(2). By the Lebesgue-Besicovitch differentiation theorem [3], $\int_{J_\gamma} T\left(w,\gamma^c\right) d\mu(w) = O\left(\mu\left(J_\gamma\right)\right) = O\left(\delta\right)$, for small $\gamma - \gamma^c > 0$. Since $\delta = O\left(\sqrt{\gamma-\gamma^c}\right)$ for $\gamma \in (\gamma^c, \bar{\gamma})$, in this region, we have $T_\gamma = T_{\gamma^c} - O\left(\sqrt{\gamma-\gamma^c}\right)$. To estimate T_γ for $\gamma > \bar{\gamma}$, we again use the proximity of P_γ to a linear map in $I - \tilde{I}$, which implies that $I - J_\gamma \approx (w_0, w_{HC} - O\left(\delta\right))$ and $d\mu(w) \approx C_2 dw$ in $I - \tilde{I}$ for some $C_2 > 0$. In addition, by the well known results of the bifurcation theory [4],

$$T\left(w,\gamma^c\right) \approx T_0 - C_3 \log\left(w_{HC} - w\right),$$

where positive constants T_0 and C_3 are independent from w, because the fast subsystem is close to a homoclinic bifurcation. Using these approximations and (11), we obtain

$$T_\gamma \approx C_2 \int_{w_0}^{w_{HC}-\delta} T\left(w,\gamma^c\right) dw \approx \bar{T} - C_4 \delta \left|\ln \delta\right| + O(\delta),$$

where positive constants $\bar{T}$ and C_6 are independent of δ and $\delta = O\left(\gamma - \gamma^c\right)$. The numerical results in Figure 5 show that the asymptotic behaviors of T_γ are different for $\gamma < \bar{\gamma}$ and $\gamma > \bar{\gamma}$. The sublinear character of T_γ in the latter region is consistent with our estimate $T_\gamma - \bar{T} = O\left(\left(\gamma - \bar{\gamma}\right)\left|\log\left(\gamma - \bar{\gamma}\right)\right|\right)$.

The map-based approach to bursting employed in this paper reduces the problem of transition from (tonic) spiking to bursting to the analysis of bifurcation scenarios in the families of the first

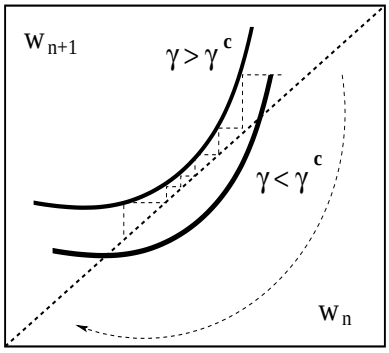

Figure 6: The mechanism of the transition to bursting through a SN bifurcation. The SN bifurcation gives rise to a periodic orbit corresponding to a bursting solution. The global return mechanism is schematically indicated by the dashed arc.

return maps. The first event in these scenarios is the loss of stability of the fixed point corresponding to tonic spiking in the continuous system. For $1D$ maps, there are two co-dimension 1 bifurcations of fixed points: a SN and a PD bifurcation [4]. The bifurcation scenario described in [7] and in the present paper originates from a PD bifurcation. A complimentary mechanism of the transition to bursting is realized through a SN bifurcation (see Figure 6). It has been recently demonstrated for a model for the leech heart interneuron [13] (see also Remark 6.1(b) in [7]). In analogy to the classification of excitability in spiking neuron models due to Rinzel and Ermentrout [10], we propose to distinguish mechanisms of transition to bursting according to the underlying bifurcation mechanisms in the families of the first return maps: **Type I** transition is realized via a SN bifurcation of the fixed point (which coincides with the global bifurcation of a periodic orbit, see Figure 6); **Type II** transition is realized through the disappearance (deflation) of the chaotic attractor (an attracting invariant interval with mixing property) preceded by a PD bifurcation. In both scenarios, the transition to bursting takes place after global bifurcations. However, the essential part of the bifurcation mechanism, which determines the traits of the bifurcating bursting patterns, in each case has a local character: a SN bifurcation in the Type I scenario and the deflation of the chaotic attractor in Type II. The bursting patterns arising through these mechanisms possess well-defined statistical properties in terms of the mean burst duration and interspike interval distributions within one burst. In particular, the interspike interval distributions in Type II bursting patterns are characterized by high variability, whereas those in Type I are localized. The mechanisms for transition to bursting in neuronal models are reminiscent to those studied in the context of the transition to turbulence via intermittency [6]. In fact, the duration of (regular) bursting near the transition in the **Type I** scenario and that of the laminar phases in the Type-I intermittency [12] share the same asymptotics due to the proximity to a SN bifurcation in both cases. In contrast, the statistical properties of the bursting patterns in **Type II** scenario are determined by the long intervals of irregular (chaotic) behavior and have not been studied before.

The author thanks to anonymous referees for insisting on careful numerical verification of the analytical estimates presented in this paper. This work was partially supported by the National Science Foundation under Grant No. 0417624.

References

[1] T.R. Chay, Chaos in a three-variable model of an excitable cell, *Physica D*, **16**, 233-242, 1984.

[2] T.R. Chay, Y.S. Fan, and Y.S. Lee, Bursting, spiking, fractals, and universality in biological rhythms, *Internat. J. of Bifurcation and Chaos*, **5**(**3**), 595–635, 1995.

[3] L.C. Evans and R.F. Gariepy, *Measure Theory and Fine Properties of Functions*, CRS Press, 1992.

[4] J. Guckenheimer and P. Holmes, *Nonlinear Oscillations, Dynamical Systems, and Bifurcations of Vector Fields*, Springer, 1983.

[5] E.M.Izhikevich, *Dynamical Systems in Neuroscience: The Geometry of Excitability and Bursting*, in press.

[6] L.D. Landau and E.M. Lifshitz, *Fluid Mechanics*, Butterworth-Heinemann, 1987.

[7] G.S. Medvedev, Reduction of a model of an excitable cell to a one-dimensional map, *Physica D*, **202**, 37-59, 2005.

[8] G.S. Medvedev and J.E. Cisternas, Multimodal regimes in a compartmental model of the dopamine neuron,*Physica D*, **194**, 333-356 , 2004.

[9] J. Rinzel, A formal classification of bursting mechanisms in excitable systems, in A.M. Gleason, ed., Proc. of the Intern. Congress of Mathematicians, AMS, 135–169, 1987.

[10] J. Rinzel and G.B. Ermentrout, Analysis of neural excitability and oscillations, in C. Koch and I. Segev, eds *Methods in Neuronal Modeling*, MIT Press, Cambridge, MA, 1989.

[11] J. Rinzel and W.C. Troy, A one-variable map analysis of bursting in the Belousov-Zhabotinskii reaction, in: J.A. Smoller, ed. *Nonlinear Partial Differential Equations*, AMS, Providence, 411–427, 1982

[12] Y. Pameau and P. Manneville, Intermittent transition to turbulence in dissipative dynamical systems, *Comm. Math. Phys.*, **74**, 1980.

[13] A. Shilnikov and G. Cymbalyuk, Transition between tonic-spiking and bursting in a neuron model via the blue-sky catastrophe, *Phys. Rev. Lett.*, **94**, 2005.

[14] Ya. G. Sinai, *Introduction to Ergodic Theory,* Princeton Univ. Press, 1976.

[15] D. Terman, The transition from bursting to continuous spiking in excitable membrane models, *J. Nonl.Sci.*, **2**, 135–182, 1992.